Microwave Remote Sensing of Falling Snow

[1]Min-Jeong Kim, [1]J. R. Wang , [1]R. Meneghini, [1]B. Johnson,
[2]S. Tanelli, [3] J.I. Roman-Nieves, [3]S. M. Sekelsky, and [1]G. Skofronick-Jackson

[1]NASA Goddard Space Flight Center, Code 975, Greenbelt, MD 20771
Phone: 301-614-6089, mjkim@neptune.gsfc.nasa.gov
[2] Atmospheric Radar Science and Engineering group Jet Propulsion Laboratory,
California Institute of Technology, Pasadena, CA 91109
[3] Department of Electrical and Computer Engineering, University of Massachusetts, Amherst, MA 01003

1. INTRODUCTION

Motivation:

Snowfall is an important component of the Earth's precipitation and hydrological cycle. Remote measurements of frozen hydrometeor properties have been limited because coincident measurements of microphysical and electromagnetic properties of snowfall have rarely been available. Ground-based radars have been widely used to monitor snowfall intensity, but even those measurements are difficult to relate to water equivalent of snow because of the vast diversity of snow habits, density, and size distributions. Moreover, the spatial coverage of radar networks is limited over most regions other than the U.S.A., Europe, and Japan.

Remote measurements at millimeter-wave frequencies can overcome this spatial/temporal sampling limitation because wavelengths are short enough to interact strongly with frozen hydrometeors and opaqueness obscures the variable emission from the underlying snow covered surface at millimeter-wave frequencies. The NOAA Advanced Microwave Sounding Unit (AMSU) has five millimeter-wave channels at 89 GHz, 150GHz, and 183.3±1 GHz, 183.3±3 GHz, and 183.3±7 GHz. The CloudSat [1] satellite, which has 95 GHz radar to measure the vertical structure of clouds from space, will be launched in summer 2005. The CloudSat will fly in the same orbit with the AQUA satellite which has passive microwave measurements at frequencies up to 89 GHz. Combining the CloudSat observations with AMSR-E and/or AMSU-B observations can shed light on snowfall measurements from space.

Challenge:

Developing a retrieval algorithm using passive and/or active microwave measurements requires parameterization of electromagnetic properties of the frozen precipitating particles to generate accurate brightness temperatures, radar attenuation, and reflectivity. However, microwave measurements of frozen hydrometeor properties were limited in the past and the electromagnetic characteristics of frozen hydrometeors are still poorly understood at present.

Research Goal:

This study analyzes passive and active microwave measurements during the 2003 Wakasa Bay field experiment for understanding of the electromagnetic characteristics of frozen hydrometeors at millimeter-wave frequencies. Based on these understandings, parameterizations of the electromagnetic scattering properties of snow at millimeter-wave frequencies are developed and applied to the hydrometeor profiles obtained by airborne radar measurements. Calculated brightness temperatures and radar reflectivity are compared with the millimeter-wave measurements.

2. OBSERVATIONS

Wakasa bay field experiment:

The U.S. AMSR-E and Japanese AMSR teams implemented a field experiment for Jan/Feb 2003 over Wakasa Bay, Japan [2]. During the field experiment, the NASA P-3 aircraft carried the dual frequency precipitation radar (PR-2) operating at 14 and 35 GHz; a cloud radar operating at 94 GHz (ACR); a passive microwave sensor (PSR) that simulates the AMSR observations; a high frequency passive Microwave Imaging Radiometer (MIR) covering from 90 to 340 GHz; and an upward looking radiometer at 21 and 37 GHz (AMMR). The Japanese contribution to the experiment consisted of a dual-polarized ground-based radar and supporting surface observations that allow us to put the aircraft observations into the larger meteorological context.

Wakasa Bay, on the eastern end of the Sea of Japan, has fairly predictable cold air outbreaks in which cold air from the Eurasian continent blows over the relatively warm Sea of Japan. These storms generally produce rainfall near the surface, where warm boundary layer air mixes with the cold air aloft. The depth of the rain layer, however, is typically very shallow and in some cases, the snowfall reaches all the way to the surface.

There were 12 flights during this field experiment between January 14 and February 3, 2003 but only one case, on January 29th, had heavy dry snow precipitation. Since the dielectric constant of liquid water is much different from air and ice, the

melting snow (air, ice, and water mixture) exhibits more complicated electromagnetic (EM) behavior than dry snow (air and ice mixture). As a first step to understand the EM scattering properties of snowfall, we therefore confine this study to dry snow retrieval only. The air temperature near the ground measured at the Fukui airport observation site during the field experiment showed that the air temperature dropped below 0°C after 23 UTC January 28th so that we assume snowfall to be dry.

Microwave measurements:

Figure 1 shows the PR-2 measured radar reflectivity at 14 and 35 GHz and the ACR measured radar reflectivity at 95 GHz over the ocean between 03 UTC and 04 UTC in January 29th, 2003. It has been reported that the center of low pressure that has been just west of Hokkaido had moved northwards to the middle of Sakhalin Island and it deepened to 979 mb. Strong northwesterly flow over all of the Sea of Japan produced extensive areas of snow off the coast during the day. Measured radar reflectivities up to 32 dBZ in the 14 GHz channel of PR-2 indicate moderate snowfall rates.

It is noted from Figure 1 that the radar reflectivities decrease with frequency, especially in the region where snowfall intensity is strong. Figure 2 shows the dual frequency ratio (DFR) between 14 GHz and 35 GHz (upper panel) and between 14 GHz and 95 GHz (lower panel). It is seen that the DFR has negative values near cloud top indicating the particles are small and backscattering properties are in Rayleigh regime. In contrast, the DFR shows large positive values where snowfall intensity is strong, especially near cloud base. This may be explained by the combination of (1) attenuation caused by snow and liquid cloud water and (2) non-Raleigh backscattering effects in the snow at the higher frequencies.

It should be noted that the DFR shows strong positive values up to the cloud top in region marked "A" in Figure 2. This shows that there is much stronger attenuation here than in other regions of the storm. The Doppler velocity measured by 14 GHz radar shown in Figure 3 indicates that the convection was very strong with vertical velocity of ~ 4.8m/s in the region. The strong vertical motion may be responsible for large amounts of supercooled cloud water and for increases in the particle size distribution. Both effects can give rise to a large DFR ratio.

Figure 4 shows the MIR measured brightness temperature (TB)s at frequencies between 89 GHz and 340 GHz. The TB depression at frequencies greater than 183 GHz is generally well correlated with the ACR and PR-2 radar reflectivity. However, the 89 GHz channel shows high TBs in many regions of the precipitation, indicating the presence of cloud water.

The retrievals of cloud liquid water with the surface reference technique (SRT) [3] using 14 GHz, 35 GHz, and 95 GHz radar reflectivity are ongoing. Retrieved cloud liquid water will be considered in radiative transfer calculations for comparison with the MIR measured TBs.
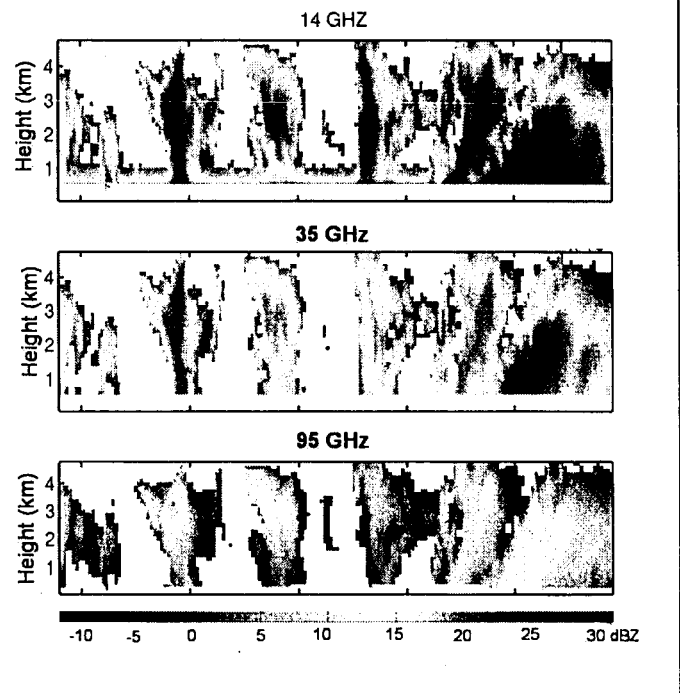

Figure 1. The PR-2 measured radar reflectivity at 14 GHz (Ku band) and 35 GHz (Ka band) and the ACR measured radar reflectivity at 95 GHz (W band) along the nadir between 03:18 UTC in January 29th, 2003.
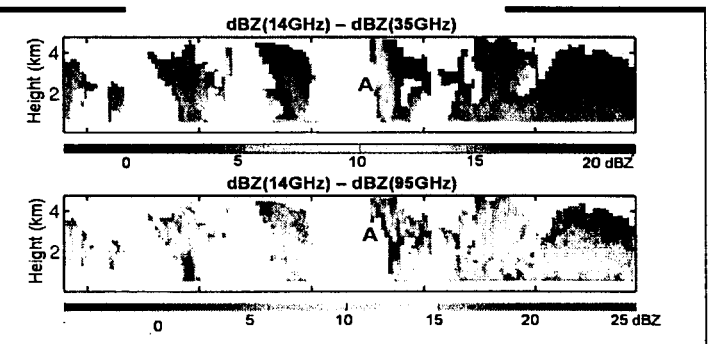

Figure 2. Dual frequency ratio (DFR) (a) for 14 GHz and 35 GHz and (b) for 14 GHz and 95 GHz along the nadir between 03:18 UTC in January 29th, 2003.
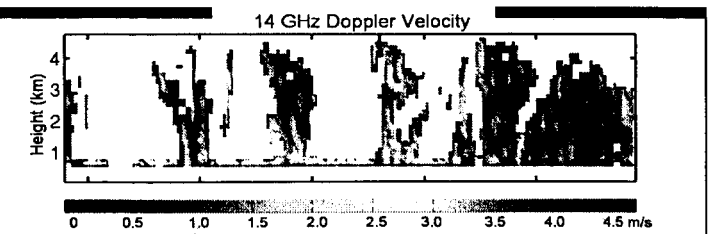

Figure 3. Doppler velocity measured by PR-2 at 14 GHz along the nadir between 03:18 UTC in January 29th, 2003.
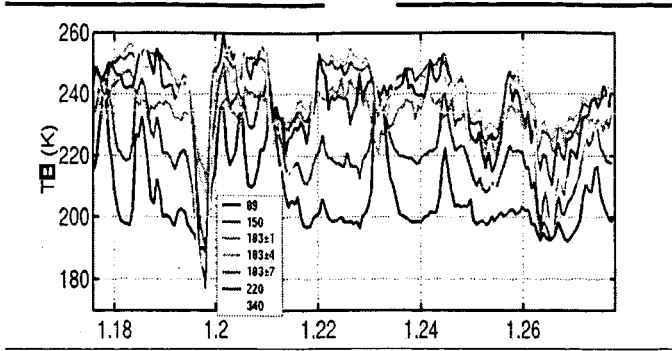
Figure 4. The MIR brightness temperatures (TB) measured at 89, 150, 183±1, 183±3, 183±7 GHz along the nadir between 03:18 UTC in January 29th, 2003.

Snow microphysics measurements:

The snow microphysics variables were measured by Kanazawa University at the ground truth site during the field experiment. Figure 4 shows snow particle size distributions (PSD) between 01-04 UTC in January 29th, 2003.
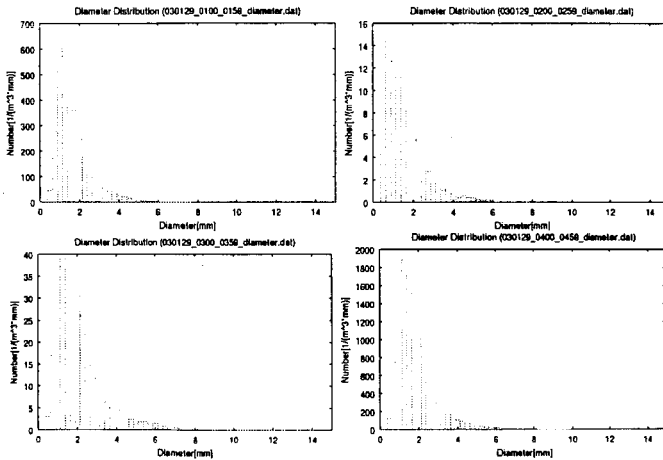

Figure 5. The snow particle size distributions measured by Kanazawa University at the ground truth site (Fukui Airport, 36.14N, 136.22 E) during the field experiment at (a) 01 UTC, (b) 02 UTC, (c) 03 UTC, and (d) 04 UTC in January 29th, 2003.

It is noted that the snow particle size distributions such as mean and maximum sizes do not change with time/snowfall intensity while the total number concentration varies from a minimum at 02 UTC (weak snowfall) to a maximum at 04 UTC (heavy snowfall). Based on these observations, the best fit gamma PSD is derived and is given by

$$N(D) = N_0 D^\mu \exp(\frac{(-3.67 + \mu)D}{D_0}) \qquad (1)$$

where D is the large dimension of a snow particle and D_0 is the median mass diameter and assumed to have a fixed value of 2.8 mm based on the observations shown in Figure 4.

3. THEORETICAL CALCULATIONS

The scattering properties depend on the morphology and orientation of snow crystals with respect to the direction of observations. Because of the variegated shapes of snowflakes, calculation of the mm-wave scattering properties is a daunting effort. Nonetheless [4] computed the scattering properties of several idealized shapes of frozen hydrometeors, such as those shown in Fig. 1, using the Discrete Dipole Approximation (DDA) described by [5] at frequencies (14, 35, 95, 140, 183, 220, and 340 GHz).
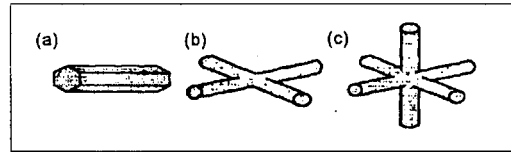

Figure 6. Snow crystal model employed in this study. (a) hexagonal column, (b) planar rosette with four arms, and (c) spatial rosettes with six arms.

Snow mass profile determined by radar reflectivity:

From the PSDs shown in Eqn.(1), snow water content profiles are derived using the PR-2 measured 14 GHz radar reflectivity assuming that at this frequency attenuation by cloud is negligible. Backscattering cross sections calculated by the DDA methods for different snow particle shapes (Fig.6) are employed. It is shown that the derived snow water content varies with the particle habit. Particles with larger mass for the same large dimension show less snow water content for a given radar reflectivity.
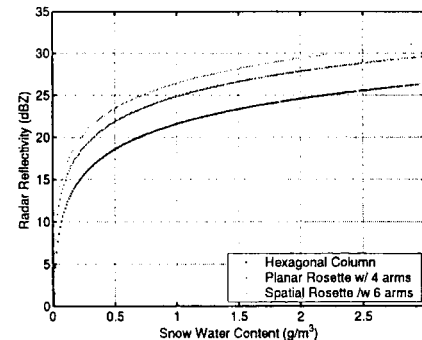

Figure 7. Snow water content derived with the DDA results for three different snow crystal shapes. The PSD in Eqn.(1) was assumed in the derivation.

Calculation of brightness temperature:

Figure 8 shows the TBs calculated with the Eddington radiative transfer model. Coincident sounding data measured during the field experiment provided the temperature, pressure,

and relative humidity profiles as well as snow profiles derived from the 14 GHz radar reflecitivity are considered in the radiative transfer calculations. The DDA calculated scattering properties are employed for each habit. It is noted that calculated TBs for hexagonal columns are much colder than the calculated TBs for spatial bullets. This is because snow water content derived from 14 GHz radar reflectivity is much higher for hexagonal columns than for aggregates like rosettes.

The results show that for most of the radiometer frequencies cold TBs are well correlated with large values of the 14GHz radar reflectivity factor. It is noted that the high 89 GHz and 150 GHz TBs observed in MIR measurements in precipitating cloud (Figure 4) could not be simulated. This may be caused by the fact that cloud liquid water was not considered in the calculations. It is expected that the addition of liquid cloud water will increase the TBs.
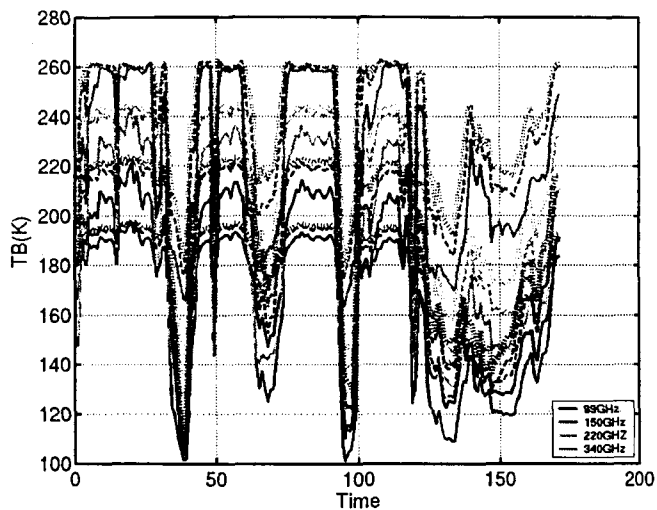

Figure 7. The Eddington radiative transfer model calculated brightness temperatures at MIR frequencies Results are shown in solid lines for hexagonal columns (Fig 6(a)), in dashed lines for planar rosettes (Fig 6(b)), and in dotted lines for spatial rosettes (Fig.6(c)).

REFERENCES

[1] Stephens, G. L., G. D. Vane, R. J. Boain, G. G. Mace, K. Sassen, Z. Wang, A. J. Illingworth, E. J. O'Connor, W. B. Rossow, S.L.Durden, S. D. Miller, R. T. Austin, A. Benedetti, C. Mitrescu, 2002: The CloudSat mission and the A-Train, Bull. Am. Meteor. Soc, 1771-1790.

[2] Wilheit, T. T., C. Kummerow, R. Ferraro, R. Austin, R. Bennartz, E. Im, and T. Bell, 2002: AMSR rainfall validation implementation strategy
http://rain.atmos.colostate.edu/Wakasa

[3] Meneghini, R., T. Iguchi, T. Kozu, L. Liao, K. Okamoto, J. A. Jones, and J. Kwiatkowski, 2000: Use of the surface reference technique for path attenuation estimates from the TRMM Precipitation Radar, J. Appl. Meteor., 39, pp 2053-2070.

[4] Kim, M.-J. 2004: A Physical model to estimate snowfall over land using microwave measurements. PhD. Thesis, Department of Atmospheric Sciences, Univ. of Washington

[5] Drain, B. T., 1988: The discrete dipole approximation and its application to interstellar graphite grains, Astrophys., J., 333, pp 848-872.